

Tco's Thin Films Grown By Spray Pyrolysis Technique For Window Layer Of Solar Cell Application: A Comparative Study

M. N. Amroun^{1,*}, K. Salim¹, A. H. Kacha² and M. Khadraoui¹

¹ Laboratoire d'Elaboration et de Caractérisation des Matériaux, département d'électronique, Université Djilali Liabes, BP89, Sidi Bel Abbès 22000. Algeria

² Laboratoire de Micro-électronique Appliquée, Université Djilali Liabès de Sidi Bel Abbès, 22000 Sidi Bel Abbès, Algeria.

Received: 2 Dec. 2019, Revised: 2 Apr. 2020, Accepted: 10 Apr. 2020

Published online: 1 May 2020

Abstract: Thin films of ZnO, SnO₂ and CdO have been deposited using spray pyrolysis technique. They were characterized by X-Ray diffraction (XRD), optical absorption in the wavelength range 200-2500 nm and Hall Effect measurements. A comparative study was conducted for the prepared TCO's thin films. The structural studies revealed the formation of polycrystalline thin films with a hexagonal wurtzite and tetragonal rutile structure for ZnO and SnO₂ thin films respectively, whereas a cubic structure was found for the CdO films. Optical studies showed that the prepared SnO₂, ZnO and CdO thin films had a direct band gap of 3.72, 2.98 and 2.43 eV, respectively. The ZnO films exhibited highest optical transmittance that varied between 70% - 88%. The film thickness of the samples was estimated from transmission spectra. The effective mass of the carriers (m^*) at the Fermi level and the figure of merit of the deposited films are also investigated. Hall Effect measurements confirm the n-type nature of the TCO's thin films. A low resistivity in the order of 10⁻² (Ω .cm) has been observed for SnO₂ and CdO thin films.

Keywords: TCO, thin films, ZnO, SnO₂, CdO, Optical constants.

1 Introduction

Transparent conducting oxide (TCO) materials have great importance in the field of thin film photovoltaic (PV) applications devices [1, 2], which have the greatest impact on the efficiency of solar cells. To improve the efficiency of a solar cell, a TCO should possess high optical transmittance across a wide spectrum and low resistivity. Furthermore, high transmittance in the visible region and wide band gap of TCOs enhance the electrical performance of PVs. Among various TCOs materials, ZnO, SnO₂ and CdO are forms of the transparent conducting oxides materials which could be deposited in the form of thin films. They are used in several applications such as solar cell [3], gas sensors [4], phototransistors [5], photodiodes [6] and transparent electrodes [7]. CdO is an n-type degenerate semiconductor with low electrical resistivity due to the presence of interstitial cadmium or oxygen vacancies, which act as doubly charged donors resulting from non-stoichiometry [8].

CdO crystallites are a simple cubic crystal system and Fm-3m space group with a lattice constant of 4.695 Å [9]. CdO has low optical band gap (2.2 eV) [10].

Tin dioxide (SnO₂) is an IV-VI oxide semiconductor with tetragonal Rutile structure. It has not only a high transparency in the visible light region but also a direct wide band gap on the order of 3.63 eV [11]. Zinc oxide (ZnO) is a promising semiconductor material from II-VI group with band gap energy of 3.37 eV, as well as a stable hexagonal wurtzite crystal structure [12].

In the present paper, the ZnO, SnO₂ and CdO films were prepared by spray technique onto glass substrates at 350°C. This technique represents a very simple processing method for preparing good quality TCO's thin films. It is easy for preparing films of any composition and does not require high quality chemicals or substrates. In the literature, it is possible to find several studies on these TCO's thin films as a window layer in solar cells application [3-10-11], but no comparative studies have been conducted these compounds. Some physical properties of the deposited ZnO, SnO₂ and CdO thin

*Corresponding author E-mail: amroun_mn@yahoo.com

films have been investigated and a comparative study carried out made for these deposited thin films.

2 Experimental Details

TCO's (ZnO, SnO₂ and CdO) thin films were synthesized using spray pyrolysis technique onto microscope glass substrates of (75×25) mm². The solution of the ZnO and CdO thin films was prepared by dissolving 0.1 M of the ZnCl₂ and CdCl₂ powder in deionized water, respectively.

SnO₂ thin films were prepared from a solution of SnCl₂ powder. The precursor was dissolved in double distilled water and methanol in volume ratio 1:1 with adding few drops of (HCl).

The substrate temperature was fixed at 350°C. Compressed air of pressure 2 bars has been used as a carrier gas, the solution flow was 8 ml/min, and spray nozzle to heating plaque distance has been fixed to 29 cm [31].

3 Results and Discussion

3.1 Structural Properties

X-ray diffraction (XRD) patterns of the prepared thin films were recorded by Philips 1830 system using Cu K α radiation ($\lambda=1.546$ Å) with 2θ in the range 20 – 70°. **Fig 1(A,B,C)** shows the X-ray diffraction (XRD) patterns of the ZnO, SnO₂ and CdO thin films deposited by spray pyrolysis method. The XRD patterns proved the polycrystalline nature of the films, which were not treated after deposition. **Fig 1(A)** exhibits that the XRD peaks observed at 32.04°, 34.62°, 36.41°, 47.74°, 56.64° and 62.94° corresponding to (100), (002), (101), (102), (110) and (103) were indexed by matching them with the JCPDS card no: 65-3411, which confirms the formation of ZnO hexagonal wurtzite structure.

Fig 1(B) illustrates the X-ray diffraction pattern of the SnO₂ films. Seven major peaks (110), (101), (200), (211), (220), (310) and (301) situate at 26.63°, 33.84°, 37.96°, 51.74°, 54.7°, 61.79° and 66.03° corresponding to the tetragonal rutile SnO₂ crystal (JCPDS No. 41-1445) were observed with the preferred orientation (110). Similar results were observed by [16]. **Fig 1(C)** manifests that the polycrystalline CdO peaks in the patterns were identified as (111), (200), (220) and (222) correspond to $2\theta = 33.07^\circ, 38.47^\circ, 55.34^\circ$ and 66.03° respectively. These peaks are consistent with the standard values of the JCPDS cards of CdO cubic structure (Card No. 05-0640) [13]. M. Anitha et al. and El Sayed et al. [14,15] also reported the similar diffraction peaks.

The lattice constants (a, b, and c) for the hexagonal, tetragonal and cubic phase structure of the deposited films ZnO, SnO₂ and CdO were defined from XRD results using the following equations, respectively [14,17,18]:

$$\frac{1}{d_{hkl}^2} = \frac{4}{3} \left(\frac{h^2 + hk + k^2}{a^2} \right) + \frac{l^2}{c^2} \quad (1)$$

$$\frac{1}{d_{hkl}^2} = \left(\frac{h^2 + k^2}{a^2} \right) + \frac{l^2}{c^2} \quad (2)$$

$$\frac{1}{d_{hkl}^2} = \frac{h^2 + k^2 + l^2}{a^2} \quad (3)$$

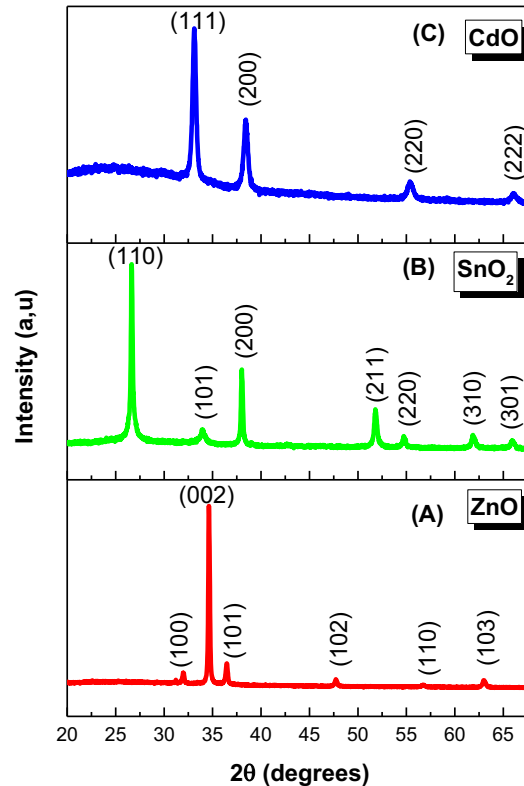


Fig. 1: XRD patterns of the deposited thin films.

The interplanar spacing d_{hkl} values of the TCO's thin films were calculated using the Bragg equation [19].

$$2 d_{hkl} \sin \theta_{hkl} = n\lambda \quad (4)$$

Where: d is interplanar spacing, (hkl) are the miller indices, λ is the wavelength, and θ is the Bragg angle. The lattice constant (a, b, and c) and interplanar spacing (d) values are listed in **Table 1**. The calculated lattice parameters of the deposited films are consistent with the standard values of the JCPDS cards of ZnO hexagonal structure (Card N°: 65-3411), SnO₂ tetragonal structure (Card N°. 41-1445) and CdO cubic structure (Card No. 05-0640).

The displacement of an atom from its lattice site (u) and bond length (L) in the (Zn:Sn:Cd)-O structure were calculated by [20]:

$$L = \sqrt{\left(\frac{a^2}{3}\right) + c^2 * (0.5 - u)^2} \quad (5)$$

$$u = \left(\frac{a^2}{3 \cdot c^2} \right) + \frac{1}{4} \quad (6)$$

Where, a and c are lattice constants of the samples. The obtained values are listed in **Table 1**.

The structural parameters, such as crystallite size (D), micro-strain (ϵ), dislocation density (δ) and stacking fault (α^*) were calculated using the following relations [19]:

$$D = (0.9 \cdot \lambda) / (\beta \cdot \cos \theta) \quad (7)$$

$$\epsilon = \frac{\beta \cdot \cos \theta}{4} \quad (8)$$

$$\delta = \frac{1}{D^2} \quad (9)$$

$$\alpha^* = \left(\frac{2\pi^2}{45(3 \tan \theta)^{1/2}} \right) \beta \quad (10)$$

Where: λ is the wavelength of Cu-K α radiation, θ is the Bragg angle and β is defined as the full width at half maximum (FWHM) of the most intense diffraction peak. The calculated crystalline parameters of the prepared films are regrouped in **Table 2**. It reveals that the CdO thin films prepared by spray pyrolysis showed the smallest crystallite size (D) in the order of 19.98 (nm) and the highest structural disorder (Strain (ϵ) = 19.10×10^{-4} , Stacking fault (α^*) = 22.11×10^{-4} (J /m²), Dislocation Density (δ) = 25.06×10^{-4} (line/nm²).

The texture coefficient TC (hkl) for predominant (002), (110) and (111) plane corresponding to the ZnO, SnO₂ and CdO films was estimated based on the following relation [21].

$$TC_{(002)} = \frac{I_{(002)} / I_{(002)}^0}{(1/N) \sum_n I_{(hkl)} / I_{(hkl)}^0} \quad (11)$$

Where I (hkl) is the measured relative intensity of a plane (hkl), I^0 (hkl) is the standard intensity of the plane (hkl) taken from the JCPDS data cited previously, N is the reflection number and 'N' is the number of diffraction peaks. The texture coefficient values (**Table 2**) of the deposited thin films greater than one (> 1) for the predominant (002), (110) and (111) plane corresponding to the ZnO, SnO₂ and CdO films are 3.98, 1.12 and 1.37 indicating a preferred orientation. The TC (111) value of the CdO films is consistent with that obtained by M.Anitha et al. [14] for CdO thin films prepared by nebulized spray pyrolysis technique.

3.2 Electrical properties

To examine the electrical properties of TCO's thin film, Hall Effect measurements are performed on all deposited films and the results are summarized in **Table 3**. The electrical parameters were measured by an automated Hall Effect system (ECOPIA HMS-5000) at room temperature. Negative value of Hall Coefficients asserts that the prepared

TCO's films are n-type conductivity. It indicates that the lowest value of the resistivity and sheet resistance 2.31×10^{-2} ($\Omega \cdot \text{cm}$) and $1.15 \times 10^{+3}$ (Ω/sq), respectively, were obtained for CdO thin films, which can be attributed to the high carrier concentrations ($1.02 \times 10^{+20} \text{ cm}^{-3}$). The low resistivity values of CdO thin films deposited by spray pyrolysis had been observed by several authors, for example, Anitha et al. ($9 \times 10^{-4} \Omega \cdot \text{cm}$) [14] and M. Azizar Rahman ($1.6 \times 10^{-4} \Omega \cdot \text{cm}$) [22]. Negative value of Hall Coefficients confirms that the prepared TCOs films are n-type conductivity.

3.3 Optical Properties

The optical measurements were carried out at room temperature in the wavelength range 200 –2500 nm using an UV-Vis-NIR (JASCO type V-570 double beam spectrophotometer). Optical transmission spectra of the prepared TCO's thin films are displayed in **Fig. 2**. The spectra of the samples indicate a large optical transmittance with an absorption edge of approximately 315 nm, 340nm and 400 nm for SnO₂, ZnO and CdO thin film, respectively. The ZnO films exhibit the highest optical transmittance varied between 70% - 88% in the visible and infrared region which can be attributed to a high structural homogeneity. The film thickness of the samples was estimated from transmission spectra. The transmission spectrum is generally divided into three regions: transparent, weakly and highly absorbing regions [23]. The transmission spectra (T) in the weakly absorbing region ($n \gg k$) can be estimated according to [29].

$$T = \frac{16 n^2 n_s X_a}{(L_1^2 + L_2^2) X_a + 2L_1 L_2 X_a \cos \varphi} \quad (12)$$

Where n is the refractive index of film, n_s is the refractive index of glass substrate and

$$L_1 = (n + 1)(n + n_s), \quad L_2 = (n - 1)(n - n_s), \quad \varphi = \frac{4\pi n d}{\lambda}, \quad X_a = \exp(-\alpha d).$$

Here α is the absorption coefficient, n_s is the refractive index of the glass substrate ($n_s = 1.51$). In the weakly absorbing region ($\alpha \neq 0$), the expression of transmission can be described as,

$T = T(n, \alpha, \lambda, d)$. However, this expression can be significantly simplified using the expression for X_a and writing the transmission as $T = \exp(-\alpha d)$ [23, 30].

Eq. (12) shows that it is possible to estimate the values of film thickness d for any point at any interference edge as long as λ is known. Hence, Eq. (12) was fitted to the transmission curve for various values of n and d until both sides are reasonably equal (**Fig 3**). The obtained values of film thickness are 210, 159 and 236 nm for ZnO, SnO₂ and CdO thin films, respectively.

Table 1: Summary of structural parameters of the deposited thin films.

Samples	Lattice constants (Å)	d spacing (Å)	L (nm)	u (nm)
ZnO	a = b = 3.228 c = 5.176	d ₍₀₀₂₎ =2.588	1.965	0.3796
SnO ₂	a = b = 4.732 c = 3.184	d ₍₁₁₀₎ =3.343	3.140	0.986
CdO	a = b = c=4.686	d ₍₁₁₁₎ =2.705	2.733	0.583

Table 2: the results and determinations using XRD data of the deposited thin films.

Samples	FWHM Peak (2θ)°	Crystallite size (D) (nm)	Dislocation Density(δ) (10 ⁻⁴ line/nm ²)	Strain (ε) (10 ⁻⁴)	Stacking fault (α*) (10 ⁻⁴ J/m ²)	texture coefficient (TC) (hkl)
ZnO	0.202	45.79	4.76	8.41	9.22	3.98
SnO ₂	0.196	46.13	4.69	8.34	9.14	1.12
CdO	0.461	19.98	25.06	19.10	22.11	1.37

Table 3: The Hall Effect results of the deposited thin films.

samples	Resistivity (ρ) (Ωcm)	Mobility (cm ² /VS)	Carrier Concentrations (cm ⁻³)	Hall Coefficient (cm ³ /C)	Sheet Resistance (Rsh) (Ω/sq)
ZnO	1.92 × 10 ⁺²	3.32	-9.74 × 10 ⁺¹⁵	-6.40 × 10 ⁺²	9.63 × 10 ⁺⁶
SnO ₂	6.04 × 10 ⁻²	0.45	-2.28 × 10 ⁺²⁰	-2.73 × 10 ⁻²	6.03 × 10 ⁺³
CdO	2.31 × 10 ⁻²	2.62	-1.02 × 10 ⁺²⁰	-6.06 × 10 ⁻²	1.15 × 10 ⁺³

The band gap energy width values were estimated from every sample adsorption edge. We have assumed from the literature that TCO thin films are characterized by direct and indirect band gap. In the case of a direct transition, the relation between the absorption coefficient (α) and the incident photon energy (hv) is given by [24].

$$(\alpha hv)^2 = A_n \cdot (hv - E_g) \quad (13)$$

Where: A_n is an energy independent constant. The direct band gap of the samples can be defined by extrapolating the linear portion of the graph as shown in **Fig. 4**. Obtained values of the direct band gap energy (E_g) of the TCO's thin films are given in **Table 4**.

The Urbach energy (E_u) which gives the width of the band tail of the localized state of the band gap can be defined by [27].

$$\alpha = \alpha_0 \exp (hv/E_u) \quad (14)$$

Where α₀ is a constant and hv is the photon energy. The Urbach energy values are estimated from the reciprocal of the slope of the linear portion of a plot of ln (α) against energy (hv). The determined values are summarized in **Table 4** which exhibits that the SnO₂ thin films shows the low degree of disorder in the film (E_u = 0.27eV), which is consistent with that previously obtained by XRD data (**Table 2**).

The effective mass of the carriers (m*) at the Fermi level of the TCO's thin films was estimated using the following relations [24, 28, 31]:

$$E = \left[\frac{h^2}{8\pi^2 \times m^*} \right] K^{*2} \quad (15)$$

$$K^* = \frac{2\pi}{\lambda_a} = \frac{2\pi \times E_a}{hc} \quad (16)$$

Where m_e is the electron of masse (9.11 × 10⁻³¹ Kg), h denotes Planck constant, E is the incident photon energy (hv), c is the speed of light, K* is the wave number, and E_a is the absorption energy of the material.

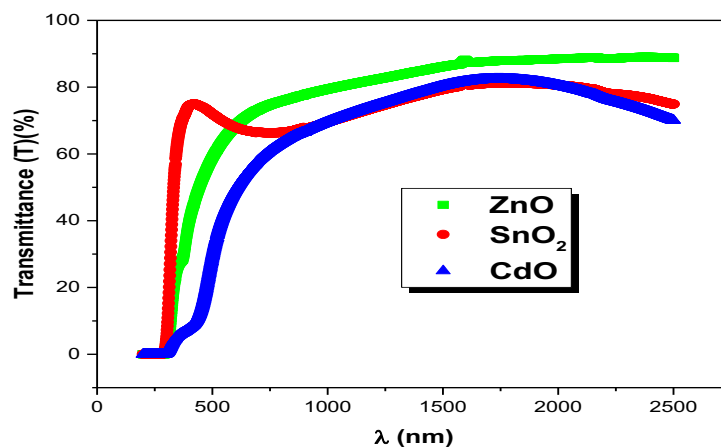


Fig. 2: Optical Transmission spectra of the deposited TCO's thin films.

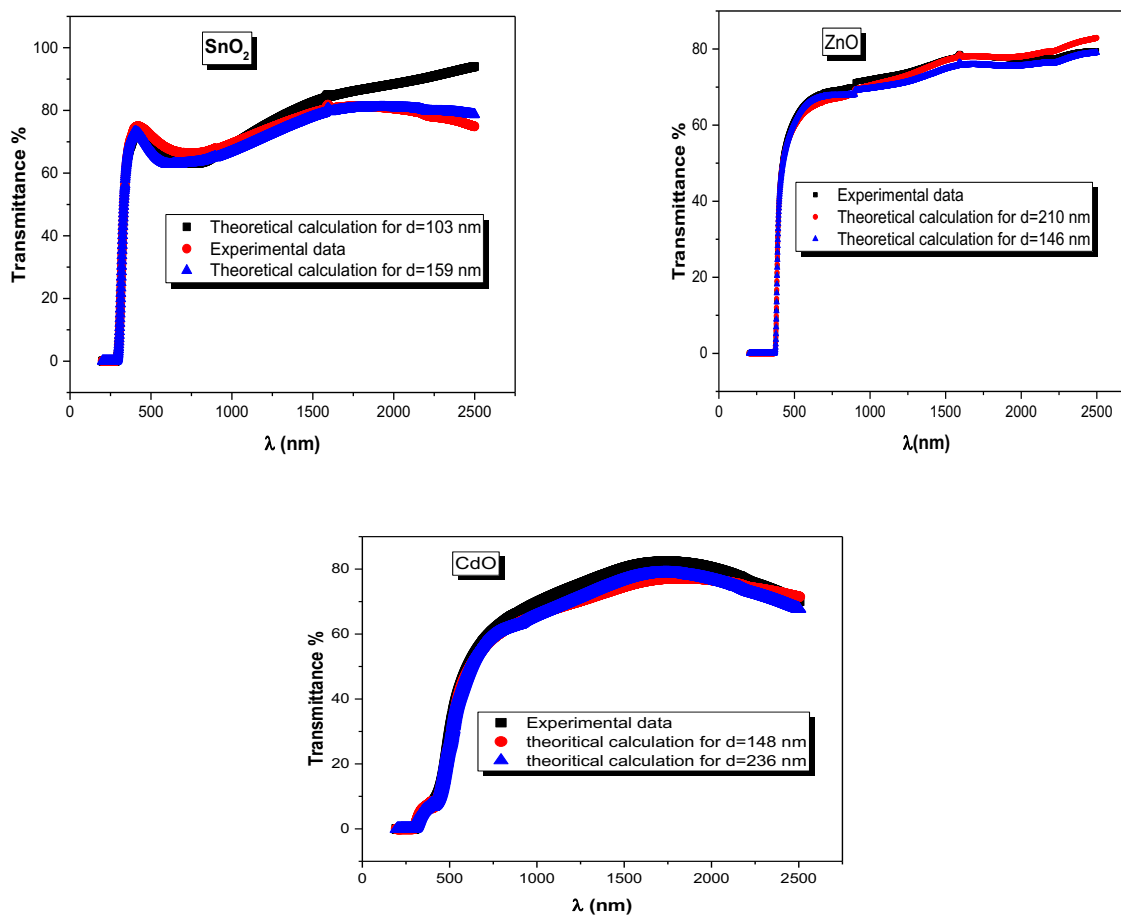


Fig. 3: Theoretical calculation and the experimental data for deposited TCO's thin films for different thickness d.

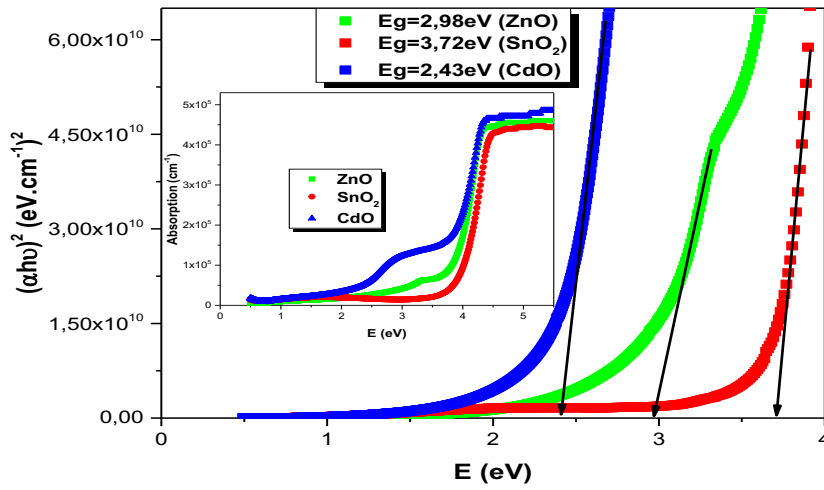
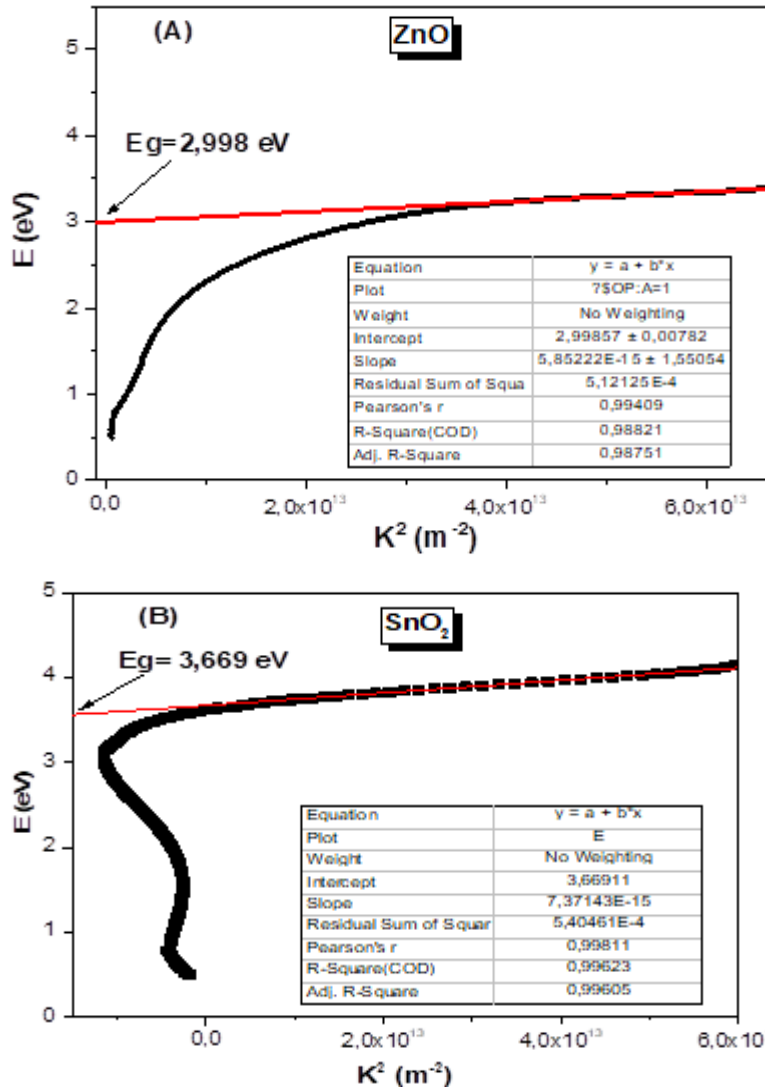


Fig. 4: plot $(\alpha h\nu)^2$ versus energy (E) of the deposited thin films.



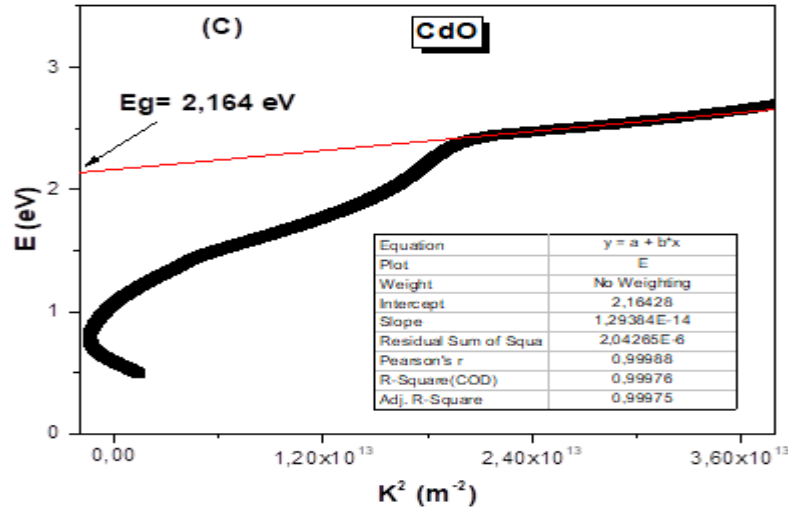


Fig. 5 (A, B, C): Photon energy E as a function of K² of the deposited thin films.

The effective mass of the carriers (m*) at the Fermi level of the prepared TCO's thin films was evaluated using the slope of the linear part in Fig 5 (A, B, C), and the obtained values are regrouped in Table 4. The extrapolation of the linear portion of the plot onto the energy axis gives an optical band gap of the ZnO, SnO₂ and CdO as 2.998 eV, 3.669 eV and 2.164 eV, respectively (see Fig 5), which is comparable with the values obtained previously from the optical absorption measurements.

The refractive index (n) is related to optical band gap (Eg) of a semiconductor by the following relation [25].

$$n = 4.084 - 0.68 E_g \tag{17}$$

Table 4 demonstrates that the refractive index (n) values of the TCO's thin film grown by spray pyrolysis technique change between 2.43 and 1.55, which is acceptable for thin layers to be used as window layers of solar cell. The lowest value of refractive index is recorded for the SnO₂ thin films because of its wide optical band gap (3.72 eV).

3.4 Optoelectronic study:

Calculation of figure of merit is to choose which TCO films present the best yield for their applications as window in solar cells. Figure of merit Φ_{TC} was defined using Haacke's formula [26]:

$$\Phi_{TC} = \frac{T}{R_{sh}} \tag{18}$$

It also exhibits that the figure of merit values in the visible and near infrared region was well observed varied between 10⁻⁴ and 10⁻⁸, and the best results are observed for CdO thin films (1.34 × 10⁻⁴) and SnO₂ (1.78 × 10⁻⁵) due to their low electrical resistivity.

4 Conclusion

The present paper addressed a comparative study of ZnO, SnO₂ and CdO thin films deposited by spray pyrolysis method. The optical and electrical structural characterization demonstrate that the thin layers of SnO₂ show less structural disorder as well as good optical and electrical parameters, such as high transmittance in the visible range > 75%, wide optical gap (Eg=3.72 eV), and low resistivity (6.04 × 10⁻² Ω.cm). These results provide a figure of merit in order of 10⁻⁵, asserting it is a potential window layer for obtaining a high efficient solar cell.

References

- [1] Gil Mo Nam and Myoung Seok Kwon, Transparent conducting Ga-doped ZnO thinfilm for flat-panel displays with a sol-gel spin coating, J. Inform. Display., 9, 8–11 (2008).
- [2] Ziad Y. Banyamin, Peter J. Kelly, Glen West, Jeffery Boardman, Electrical and optical properties of fluorine doped tin oxide thin films prepared by magnetron sputtering, Coatings., 4, 732–746 (2014).
- [3] B. Saha, S. Das, K.K. Chattopadhyay, Electrical and optical properties of Al doped cadmium oxide thin films deposited by radio frequency magnetron sputtering, Sol. Energy Mater. Sol. Cells., 91, 1692–1697(2007).
- [4] R.R. Salunkhe, D.S. Dhawale, D.P. Dubal, C.D. Lokhande, Sprayed CdO thin films for liquefied petroleum gas (LPG) detection, Sens. Actuators., B 140, 86–91(2009).

- [5] L.M. Su, N. Grote, F. Schmitt, Diffused planar InP bipolar transistor with a cadmium oxide film emitter, *Electron. Lett.*, **20**, 716–717 (1984).
- [6] R. Kondo, H. Okimura, Y. Sakai, Electrical properties of semiconductor photodiodes with semi-transparent films, *Jpn. J. Appl. Phys.*, **10**, 1547 (1971).
- [7] W.M. Cho, G.R. He, T.H. Su, Y.J. Lin, Transparent high surface work function Al-doped CdO electrodes obtained by rf magnetron sputtering with oxygen flow, *Appl. Surf. Sci.*, **258**, 4632–4635 (2012).
- [8] L.L. Pan, G.Y. Li, J.S. Lian, Structural, optical and electrical properties of cerium and gadolinium doped CdO thin films, *Appl. Surf. Sci.*, **274**, 365–370 (2013).
- [9] Powder Diffraction File, International centre for Diffraction data, Reference code: 00-005-0640.
- [10] K.L. Chopra, S. Ranja, *Thin film solar*, Cells Newyork (1993).
- [11] Chafia Khelifi, Abdallah Attaf, Hanane saidi, Anouar Yahia, Mohamed Dahnoun, Investigation of F doped SnO₂ thin films properties deposited via ultrasonic spray technique for several applications *Surfaces and Interfaces.*, **15**, 244–249 (2019).
- [12] A.A. Othman, M.A. Osman, E.M.M. Ibrahim, Manar A. Ali, A.G. Abd-Elrahim, *Materials Science and Engineering B.*, **219**, 1–9 (2017).
- [13] JCPDS – International Centre for Diffraction Data, Card No. 05-0640, (1997).
- [14] M. Anitha, K. Saravanakumar, N. Anitha, I. Kulandaisamy, L. Amalraj, Influence of annealing temperature on physical properties of Sn-doped CdO thin films by nebulized spray pyrolysis technique, *Materials Science & Engineering B.*, **243**, 54–64 (2019).
- [15] A.M. ElSayed, Ali Ibrahim, Structural and optical characterizations of spin coated cobalt-doped cadmium oxide nanostructured thin films, *Mater. Sci. Semicond. Process.*, **26**, 320–328 (2014).
- [16] Xu Zhang, Xianzhe Liu, Honglong Ning, Weijian Yuan, Yuxi Deng, Xiaochen Zhang, Shuang Wang, Jialiang Wang, Rihui Yao, Junbiao Peng. Characterization studies of the structure and properties of Zr-doped SnO₂ thin films by spin-coating technique, *Superlattices and Microstructures.*, **123**, 330–337 (2018).
- [17] M.N. Amroun, M. Khadraoui, R. Miloua, N. Benramdane, K. Sahraoui, Z. Kebbab, *Journal of Optoelectronic and Advanced Materials.*, **19**, 771 – 777 (2017).
- [18] Boubaker Benhaoua, Soumaia Abbas, Achour Rahal, Atmane Benhaoua, M.S. Aida, Effect of film thickness on the structural, optical and electrical properties of SnO₂: F thin films prepared by spray ultrasonic for solar cells applications, *Superlattices and Microstructures.*, **83**, 78–88 (2015).
- [19] M.N. Amroun, M. Khadraoui, Effect of substrate temperature on the properties of SnS₂ thin films, *Optik.*, **184**, 16–27 (2019).
- [20] D. Akcan, A. Gungor, L. Arda, *Journal of Molecular Structure.*, **1161**, 299e305 (2018).
- [21] Chafia Khelifi, Abdallah Attaf, Hanane saidi, Anouar Yahia, Mohamed Dahnoun, *Surfaces and Interfaces.*, **15**, 244–249 (2019).
- [22] M. Azizar Rahman, M.K.R. Khan, Effect of annealing temperature on structural, electrical and optical properties of spray pyrolytic nanocrystalline CdO thin films, *Mater. Sci. Semicond. Process.*, **24**, 26–33 (2014).
- [23] E.R. Marquez, J. Malo, P. Villares, G.R. Jimenez, S.P. Ewen, A.E. Owen, Calculation of the thickness and optical constants of amorphous arsenic sulfide thin films from their transmission spectra, *J. Appl. Phys. D.*, **25**, 535–541 (1992).
- [24] Amroun MN, Khadraoui M. *Int J Numer Model.*; e 2617. <https://doi.org/10.1002/jnm.2617> (2019).
- [25] N. M. Ravindra, *Infrared phys. and technology.*, **21** 283–285 (1981).
- [26] M. Anitha, V. Tamilnayagam, N. Anitha, L. Amalraj, S. Gokul Raj, *J. Mater. Sci.: Mater. Electron.*, **28** 17297–17307 (2017).
- [27] M.N. Amroun, M. Khadraoui, R. Miloua, Z. Kebbab, K. Sahraoui, Investigation on the structural, optical and electrical properties of mixed SnS₂—CdS thin films, *Optik.*, **131**, 152–164 (2017).
- [28] N. Koteeswara Reddy, K.T. Ramakrishna Reddy, *Materials Research Bulletin.*, **41**, 414–422 (2006).
- [29] K.S. Pramod, V.K. Varadan, V.V. Varadan, Optical, dielectric and fatigue properties of sol–gel-derived 2 μm thick Pb (Zr_{0.53}Ti_{0.47})O₃ ferroelectric films, *Smart Mater. Struct.*, **11**, 956–961 (2002).
- [30] J.C. Manifacier, J. Gasiot, J.P. Fillard, A simple method for the determination of the optical constants n, k and the thickness of a weakly absorbing thin film, *J. Phys. E Sci. Instrum.*, **9**, 1002–1004 (1976).
- [31] M.N. Amroun et al. Effect of TM (TM= Sn, Mn, Al) Doping on the Physical Properties of ZnO Thin Films Grown by Spray Pyrolysis Technique: A comparative Study. *Int. J. Thin.Film. Sci. Technol.* <http://dx.doi.org/10.18576/ijtfst/>, **9(1)**, (2020).